Thermochimica Acta, 37 (1980) 53—64

THE USE OF COMPOSITE BEAMS TO MEASURE THE DYNAMIC MECHANICAL PROPERTIES OF SEMI-RIGID SOLIDS

R.P. KUSY and A.R. GREENBERG

Dental Research Center, University of North Carolina, Chapel Hill, N.C. 27514 (U.S.A.)

(Received 8 August 1979)

ABSTRACT

The theoretical foundation of dynamic thermomechanometry is expanded to include the relaxation of another class of materials, that of semi-rigid solids. By transforming composite beams into homogeneous beams, an expression for the sample modulus (E_s) is derived

$$E_s = \frac{2\pi^2 J(f_c^2 - f_h^2)}{w(D + \frac{1}{2}L)^2}\left(\frac{L}{t}\right)^3$$

and the general relationship between the shape factor, the elastic constants, and the moment of inertia set forth. Using dental amalgam as a test case, the modulus of five alloys was determined as a function of time and ranged from 3.9 to 6.6 × 10^{10} Pa after ~15 h. These values were greater than conventional compression tests but less than ultrasonic experiments. Potential sources of errors in the technique are explored, and the general state of the art reviewed.

INTRODUCTION

Over the last 40 years many instruments have been developed to measure the relaxation properties of materials. Amongst the more popular types have been the torsion pendulum, the vibrating reed, and the rotating beam systems [1]. Each apparatus, whether its nature be forced vibration or free-frequency resonance, has a particular physical state, temperature, and frequency range over which the most reliable modulus values can be obtained.

Recently, another mechanical spectroscopy technique has been introduced [2] that resonates a compound parallel beam system about two flexure pivots using a sample coupling arrangement (cf. Fig. 1). Via the 90° phase-locked, fixed amplitude driving system, a characteristic frequency and damping response are measured, from which modulus and tan δ data can be derived. To date, expressions have been reported for determining either a Young's (E) or shear (G) modulus [2,3]. In addition, samples have been investigated in both the solid and liquid state — the former using a ribbon-like or slender beam geometry, while the latter employing a coil spring or a woven fabric as a substrate.

The current effort considers the problem of measuring the elastic moduli of semi-rigid solids. This classification encompasses materials which at some

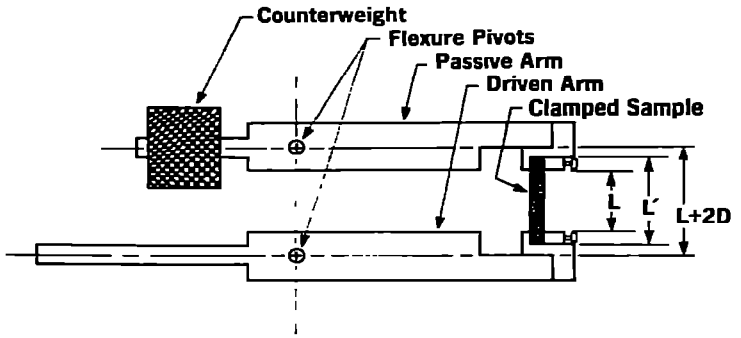

Fig. 1. Schematic illustration of the compound resonant system showing the relationship of the sample to the oscillating parallel arms.

stage of testing are too viscous to be treated as fluids and yet not stiff enough to be self-supporting beams. In the early stages of setting cements, aggregates, and amalgams are prime examples of such materials. Following the theoretical development of the composite beam approach, dental amalgams will be employed to demonstrate the application of the derived equations.

GENERAL CONSIDERATIONS

From the schematic drawing of Fig. 1, the balanced driven and passive arms may be considered as simple harmonic oscillators. Analogous to linear harmonic motion, the angular harmonic motion may be described by a similar set of equations [4] where the restoring torque (Γ) is proportional to the angular displacement from the rest position (ϕ) or

$$\Gamma = -K\phi \tag{1}$$

Here K is called the torque constant. If friction is negligible the differential equation of motion is

$$J\frac{d^2\phi}{d\tau^2} + K\phi = 0 \tag{2}$$

(J being the moment of inertia of the rotating body), a general solution of which equals

$$\phi = B \sin\left(\sqrt{\frac{K}{J}}\,\tau + \phi_0\right) \tag{3}$$

Since the angle, $(\sqrt{K/J}\,\tau + \phi_0)$, is the same at time τ as it is after one period $(1/f)$

$$\sqrt{\frac{K}{J}}\left(\tau + \frac{1}{f}\right) + \phi_0 = \sqrt{\frac{K}{J}}\,\tau + \phi_0 + 2\pi$$

and

$$f = \frac{1}{2\pi}\sqrt{\frac{K}{J}} \tag{4}$$

Now as the free-body diagrams show (Fig. 2a, b), several torques act on both arms. By summing these moments about their respective pivot points, however, the restoring torque is easily found for the passive arm

$$\Gamma = M_p + M_s + VD - CR = -K\phi = J\frac{d^2\phi}{d\tau^2} \tag{5}$$

and

$$\Gamma = M_p - M_s + V(D + L) + CR = -K\phi = (J + m_s R^2)\frac{d^2\phi}{d\tau^2} \tag{6}$$

for the driver arm/sample combination. Since the mass of the sample (m_s) and its associated moment of inertia is negligible compared to that of the driven arm itself, the net restoring torque of the compound resonant system can be written as

$$J\frac{d^2\phi}{d\tau^2} - \left(M_p + VD + \frac{VL}{2}\right) = 0 \tag{7}$$

The pivot's moment (M_p) and the shear force (V) can be evaluated from the free-body diagram for the sample (Fig. 2c) by double integration of the differential equation of the elastic curve of a beam, i.e.

$$M = EI\frac{d^2y}{dx^2} \tag{8}$$

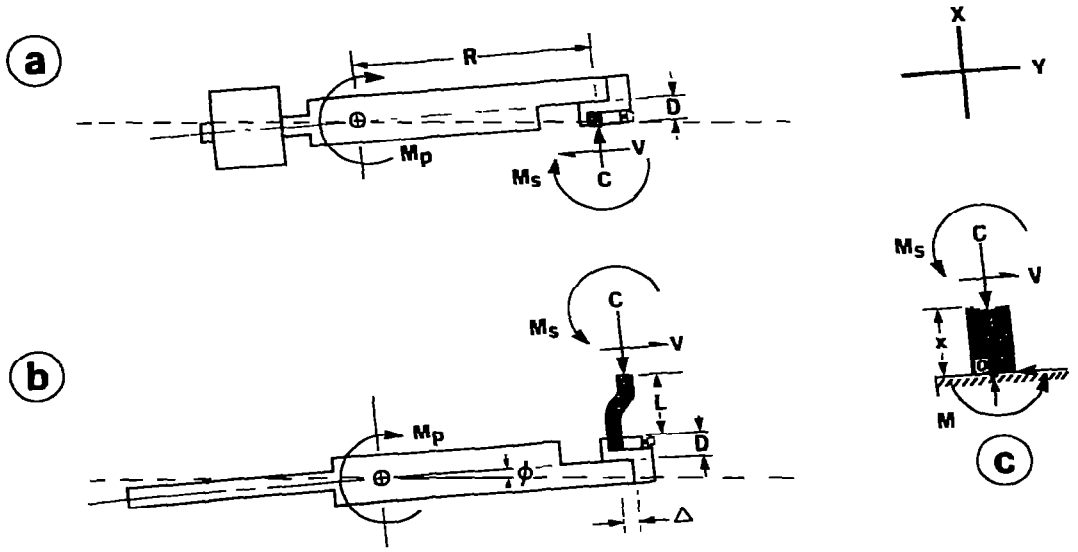

Fig. 2. Free-body diagrams. (a) Passive arm, (b) driven arm/sample combination; and (c) sample.

where I is the moment of inertia [5]. By setting $\Sigma M_0 = 0$

$$M = Vx - M_s \tag{9}$$

and one obtains

$$\frac{d^2y}{dx^2} = \frac{1}{EI}(Vx - M_s) \tag{10}$$

$$\frac{dy}{dx} = \frac{1}{EI}\left(\frac{Vx^2}{2} - M_s x\right) + C_1 \tag{11}$$

and

$$y = \frac{1}{EI}\left(\frac{Vx^3}{6} - \frac{M_s x^2}{2}\right) + C_1 x + C_2 \tag{12}$$

where C_1 and $C_2 = 0$. From eqn. (11) and the boundary condition that $dy/dx = 0$ at $x = L$

$$M_s = \frac{VL}{2} \tag{11a}$$

while from eqn. (11a) and the boundary condition that $y = \Delta$ at $x = L$, eqn. (12) yields V

$$V = -\frac{12EI\Delta}{L^3} \tag{12a}$$

As the driven arm rotates through an angle ϕ, the intersection of the long axes of each beam with the clamped axis of the sample rotate similarly. Since both ϕ and the flexural rigidity of the sample relative to the beams are small, the displacement of these points with respect to the sample in the y-direction equal

$$\Delta \doteq (2D + L)\,\phi \tag{13}$$

By substitution of V (eqn. 12a), Δ (eqn. 13), and the moment of the pivot ($M_p = -K_p\phi$) into eqn. (7), eqn. (14) results

$$J\frac{d^2\phi}{d\tau^2} + \left[K_p + \frac{24EI(D + \frac{1}{2}L)^2}{L^3}\right]\phi = 0 \tag{14}$$

Comparing eqn. (14) with eqn. (2), the analog to eqn. (4) can be stated as

$$f = \frac{1}{2\pi}\left[\frac{K_p + (24EI(D + \frac{1}{2}L)^2)/L^3}{J}\right]^{1/2} \tag{15}$$

HOMOGENEOUS BEAMS

Solution of eqn. (15) may be solved for the case of simple sample beams if the following assumptions are valid [6]:

(1) the beam is straight and has a uniform cross-sectional area;

(2) E is invariant over the cross-section and in all directions, i.e., the beam is both homogeneous and isotropic (this implies that the material obeys Hooke's law, and that E is the same for tension as for compression);

(3) the beam does not warp, twist, or buckle as a result of bending. To satisfy this requirement an axis of symmetry of the beam should lie in the plane of loading;

(4) the loads applied are equivalent to a pure moment.

When these conditions are approached, the moduli for any geometry may be considered — whether they be common shapes (e.g., squares, rectangles, triangles, or circles), or more intricate cross-sections (e.g., hollow squares, quarter circles, or extruded channels). In any case, the moment of inertia about the neutral axis need only be substituted in eqn. (15), along with the experimentally determined K_p and J, to obtain E. For example, for the case of a rectangular prism being flexed in the plane indicated in Fig. 3(a)

$$I = \frac{WT^3}{12} \tag{16}$$

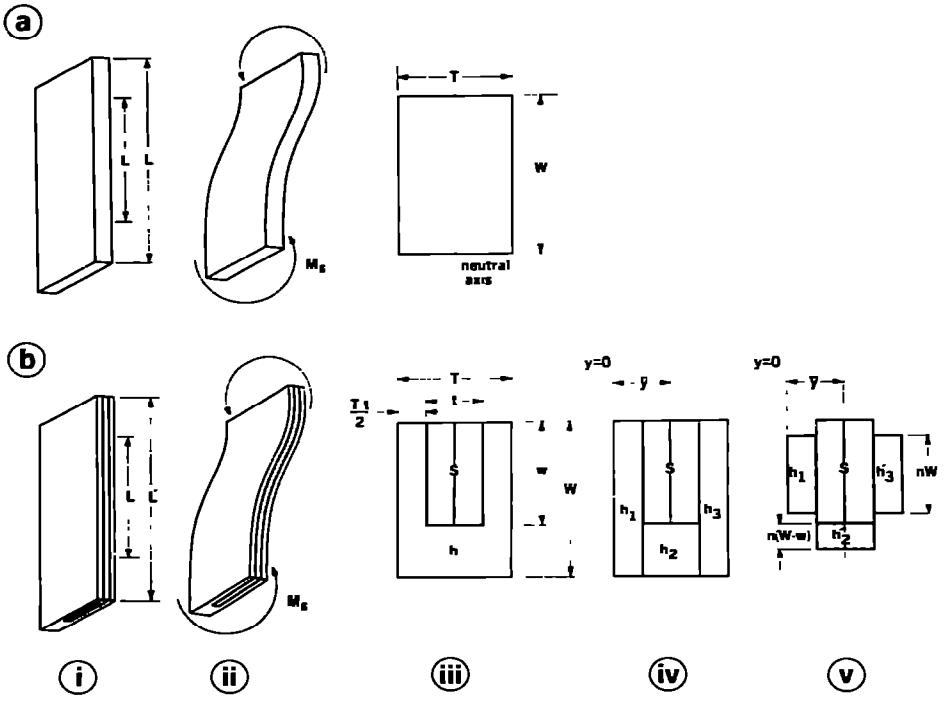

Fig. 3. Geometry of (a) homogeneous and (b) non-homogeneous beams. (i), Over-view of unstressed and (ii) flexed member (cf. Figs. 1 and 2b); (iii), actual cross-sectional area, (iv), area (iii) partitioned; and (v), area (iv) transformed.

and

$$E = \left[\frac{4\pi^2 f^2 J - K_p}{2W(D + \frac{1}{2}L)^2}\right]\left(\frac{L}{T}\right)^3 \tag{17}$$

This expression will be useful for comparison with the compound beam case that follows.

NON-HOMOGENEOUS BEAMS

In order to evaluate semi-rigid materials, a superstructure must be fabricated from a resilient, non-reactive material that responds predictably under test conditions. To insure a good sample frequency response, the ratio of the flexural rigidity (EI) of the sample (s) to the holder (h) should be maximized. However, since the holder is more remote from the neutral axis of the composite beam, I_h increases at a substantially greater rate than I_s. Because the superstructure must be sufficient enough to support the sample, I_h must inevitably represent a compromise between signal response and function. Therefore, only if E_h can be reduced can the sample represent a significant portion of the compound beam signal.

The preceding criterion, that the sample and holder be composed of materials of different moduli of elasticity, constitutes a non-homogeneous beam. Solution to such a problem requires that all materials of the original section be transformed into an equivalent beam of one material. This transformation approach may be used if there is no slip between dissimilar materials [6]. Thereafter the transformed cross-sectional area of the new beam may be evaluated as a homogeneous beam by elastic theory.

As a general case, consider the composite beam of Fig. 3(b). Here the cross-section of the sample (s) and U-shaped holder (h) may be described in terms of the thickness (t, T) and width (w, W) dimensions, respectively. By partitioning the U-shaped channel into three components — h_1, h_2, and h_3 — the actual section is ready to be transformed from either s into h or h into s. Choosing the latter, n is defined as

$$n = E_h/E_s \tag{18}$$

and the transformed section is generated. Because of symmetry, the neutral axis of the transformed section is located at the mid-depth of the beam; that is, the centroid ($\bar{y}$) of the partitioned section relative to the transformed section is unchanged *. Using $\bar{y} = T/2$, the moment of inertia of the trans-

* However, if the beam had been flexed around an asymmetrical plane — e.g., the perpendicular axis — a new centroidal distance

$$\bar{y} = \frac{\sum_{h=1}^{i} n(A_h y_h) + \sum_{s=1}^{j} (A_s y_s)}{\sum_{h=1}^{i} nA_h + \sum_{s=1}^{j} A_s}$$

would have had to have been defined by substitution of the cross-sectional area (A) and the distance (y) from an arbitrary reference point for each component (h or s).

formed section equals

$$I = \sum_{h=1}^{i} n(I_{h_{cent.}} + A_h d_h^2) + \sum_{s=1}^{j} (I_{s_{cent.}} + A_s d_s^2) \tag{19}$$

where $I_{cent.}$ is the moment of inertia of a component about its centroid, and d is the distance of the centroid of a component from the centroid of the transformed section. Accordingly, the total moment of inertia of the composite beam (I_c) equals

$$I_c = nI_{h_1} + nI_{h_2} + nI_{h_3} + I_s = I_{h'_1} + I_{h'_2} + I_{h'_3} + I_s \tag{20}$$

where

$$I_{h'_1} = \frac{nW[\frac{1}{2}T - t)]^3}{12} + nW\left(\frac{T-t}{2}\right)\left(\frac{t}{2} + \frac{T-t}{4}\right)^2 \tag{20a}$$

$$I_{h'_2} = \frac{n(W-w)\,t^3}{12} \tag{20b}$$

$$I_{h'_3} = I_{h'_1} \tag{20c}$$

and

$$I_s = \frac{wt^3}{12} \tag{20d}$$

Combining eqns. (20a—d)

$$I_c = \tfrac{1}{12}[n(WT^3 - wt^3) + wt^3] \tag{21}$$

from which

$$I_c/I_s = [1 + n(\beta\alpha^3 - 1)] \tag{21a}$$

when $\alpha = T/t$ and $\beta = W/w$. Figure 4 summarizes the effect that the shape factor ($\beta\alpha^3$) has on I_c/I_s for several values of n.

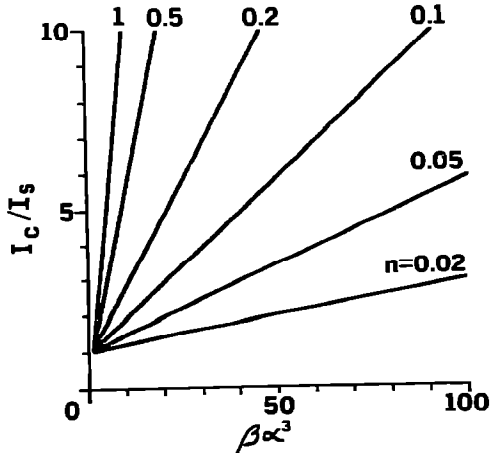

Fig. 4. Relationship of shape factor ($\beta\alpha^3$) and moduli ratio (n) to the quotient of the composite and sample beams' moments of inertia (I_c/I_s).

Having transformed the composite section into an equivalent beam of one material, eqn. (21a) can be substituted into eqn. (15), giving the frequency response of the equivalent composite beam (f_c) as

$$f_c = \frac{1}{2\pi}\left\{\frac{K_p + \{[24E_sI_s[1 + n(\beta\alpha^3 - 1)](D + \frac{1}{2}L)^2]/L^3\}}{J}\right\}^{1/2} \tag{22}$$

and since by a similar analysis

$$I_h/I_s = (\beta\alpha^3 - 1) \tag{23}$$

the frequency response of the holder alone (f_h) can be expressed from eqns. (15) and (23) as

$$f_h = \frac{1}{2\pi}\left\{\frac{K_p + \{[24E_hI_s(\beta\alpha^3 - 1)(D + \frac{1}{2}L)^2]/L^3\}}{J}\right\}^{1/2} \tag{24}$$

Substitution of eqns. (18), (20d) and (24) into eqn. (22) yields

$$E_s = \frac{2\pi^2 J(f_c^2 - f_h^2)}{w(D + \frac{1}{2}L)^2}\left(\frac{L}{t}\right)^3 \tag{25}$$

Thus by knowing the distance between the pivot arms, the moment of inertia of the arms, and the geometry of the sample outside the sample clamps, the modulus of the sample may be obtained by simply measuring the frequency response of the holder with and without the sample present; and unlike the homogeneous beam case (eqn. 17), no K_p need be determined in eqn. (25) since relative differences are being considered.

THE EXPERIMENT

Immediately after trituration and condensation, dental amalgam (henceforth designated by the subscript a) is a semi-rigid solid. Although some of the newer ternary alloys do harden enough after 1 h to enable a patient to apply significant forces of mastication [7—9], even these alloys are not able to withstand the clamping stresses that self-supporting beams would experience initially. Moreover, in addition to the diametral tensile, compressive, and flow tests that are commonly used to evaluate the early setting characteristics of amalgam [7—12], the reaction of the mercury with the other alloy constituents (primarily silver and tin) does result in gross phase changes that should affect the elastic constants. Hence, dynamic thermomechanometry might further clarify the early setting behavior of these alloys.

Five different amalgams were prepared: two commercial spherical ternary alloys (1 and 2), an experimental modified spherical ternary alloy (3), a commercial improved lathe-cut binary alloy (4) and an experimental monodisperse spherical binary alloy (5). After adding alloy powder to mercury in the specific weight ratio (44—50% Hg) and after trituration for 8—25 sec in a high speed amalgamator, each alloy was condensed into a reinforced U-shaped poly(methyl methacrylate) channel (Plexiglas G, Rohm and Haas Co.,

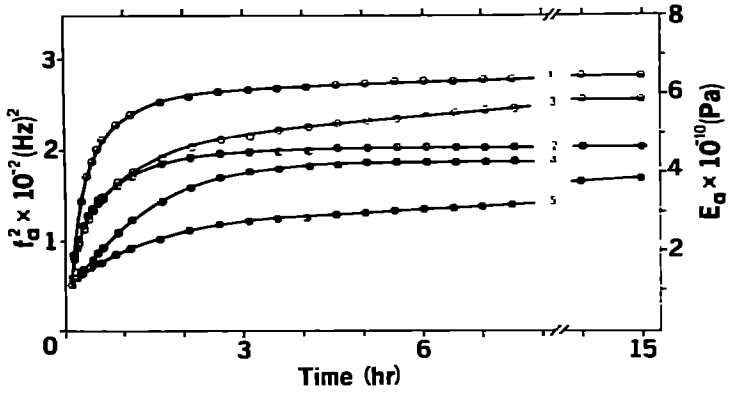

Fig. 5. Early setting time dependence of five dental amalgams via dynamic mechanical measurements. Modulus values were determined directly from eqn. (25).

Philadelphia, Pa.). Acrylic was selected for the superstructure because it is an unreactive, transparent, low modulus ($E_h \approx 2.8 \times 10^9$ Pa) material that is frequently used as a machine calibration standard. Overall dimensions for the unclamped (L′) and clamped (L) composite beam were 30.5 and 17.8 mm, respectively, while the cross-sectional specifications were $T = 2.0$ mm, $t = 1.0$ mm, $W = 3.0$ mm, and $w = 2.0$ mm (cf. Fig. 3b) for an $L/T = 9$. For the shape factor $\beta\alpha^3 = 12$ and an estimated final $n \approx 0.1$—0.05, Fig. 4 indicated that the sample represented from 1/2 to 2/3 of the total composite beam moment of inertia. The resulting high output signals were essential if sufficient resolution was to be realized at early times when the n was approximately five times greater, i.e., when I_a equalled 1/6—1/3 of I_c. Within 5—7 min after the start of trituration, the composite beam was clamped into the compound resonant system of a DuPont 981 Dynamic Mechanical Analyzer and the frequency (f_c) continuously monitored at 37°C after setting the oscillator amplitude (Δ) and A/Z gain to 0.20 mm and 0.35, respectively. Having determined f_h for each empty holder under the identical operating conditions as for f_c, and having measured the system constants for this instrument ($J = 1.61 \times 10^{-3}$ kg m^2 and $D = 9.93 \times 10^{-3}$ m), E_a was computed from eqn. (25).

Results for the five alloys within the first 15 h of setting are shown in Fig. 5. Initially $f_c \approx 12$ Hz vs. $f_h \approx 10$ Hz for a modulus of 1.2×10^{10} Pa — a value ca. 4 times greater than the PMMA holder alone. Soon thereafter, however, differences in alloy composition, particle size or shape, or processing treatment affected the setting reaction rates, thereby changing the moduli. In the present case, the ternary alloys are seen to attain one-half of their 15 h moduli in ~15 min, compared to the monodisperse alloy that required a factor of 4 more time. This observation suggests that a more rapid rate of moduli change would be expected to result in superior early strength properties. Indeed, the hypothesis is corroborated by the data of Malhotra and Asgar [8], who observed that two ternary dental alloys yielded 1 h, compressive strengths that were from 50 to 700% greater than those obtained on five conventional amalgams. Returning again to Fig. 5, with the exception of

alloy 5, the 15 h moduli are approaching their maxima at 3.9—6.6 × 10^{10} Pa. In the literature, moduli values for amalgam and its constituent phases span a considerable range (0.7—8.3 × 10^{10} Pa) due to differences in test instrumentation, strain rate, and sample preparation [13—21]. However, because of the viscoelastic nature of the material itself, the most reliable estimates must be the low stress, high strain rate tests, i.e., the pulsed ultrasonic techniques [17—19]. Here both Dickson and Oglesby [17] and Grenoble and Katz [18] have measured Young's moduli of 6.3—6.9 × 10^{10} Pa for bulk amalgam samples with 50% Hg by weight, although individual phases may be as low as 4.9 × 10^{10} Pa [19]. The present technique only approaches those values obtained by ultrasonics, although it generally yields results superior to those reported using standard tensile or compressive tests [13—16,20,21]. Recently, measurements on micro-compression specimens fabricated from these same dynamic mechanical spectroscopy beams gave E_a = 4.1—5.4 × 10^{10} Pa [22].

SPECIAL CONSIDERATIONS

As Fig. 3b shows, an axis of symmetry of the composite beam does not lie in the plane of loading. As previously stated, however, some departure from the assumptions inherent in homogeneous beam theory may be accommodated without serious errors. For the current experiment the magnitude of the error caused by this asymmetry can be estimated by considering the contribution of component h_2' to the transformed section. By substituting the dimensions for the composite beam into eqn. (20)

$$I_c = [I_{h_1'} + I_{h_3'}] + [I_{h_2'}] + [I_a] = \left[\frac{7n}{4}\right] + \left[\frac{n}{12}\right] + \left[\frac{1}{6}\right] \text{ mm}^4$$

Clearly h_2' always contributes ~5% to the overall moment of inertia of the holder and a lesser percentage compared to the sample when $n < 0.1$. In fact, not until $n \geqslant 0.3$ does $I_{h_2'} \geqslant 0.15\ I_a$. Considering these circumstances, the holder's asymmetry is more beneficial toward maintaining the superstructure's geometry during condensation and in preventing slip during dynamic testing than it is deleterious.

Although the sample's moment of inertia ($m_s R^2$) was neglected early in the general derivation (cf. text following eqn. 6), that assumption must be verified for the present experiment by comparing the composite beam's moment of inertia ($m_c R^2$) to the moment of inertia of the arms ($2J$). When $m_c = 2.35 \times 10^{-3}$ kg and $R = 0.112$ m, $m_c R^2$ represented less than 0.01 ($2J + m_c R^2$).

CLOSING COMMENTS

Although dynamic thermomechanometry can yield qualitative data on similar samples — e.g., in quality control situations — quantitative results require special attention. For the case of either homogeneous or transformed

non-homogeneous beams, three factors must be considered: the aspect ratio in the bending plane (L/T), the flexural rigidity (EI), and the oscillation amplitude (Δ). To avoid both shear and bending moduli components from being present, L/T must be ≤ 1 for the shear modulus situation (G) and $8 \leqslant L/T \leqslant \epsilon$ for E. While in the bending case the upper limit of L/T is not stated, certainly one exists; since when T becomes thin enough, localized wrinkling or buckling would occur. Similarly the lower limit of EI is set either by this critical thickness or by the loss of sample to baseline signal resolution. And as was the case for L/T an upper limit must exist for EI, too, as the sample's stiffness or its associated internal friction becomes so great that either the electromagnetic feedback system is unable to drive the compound resonant system at the prescribed Δ or the differential equation of motion eqn. (2) no longer applies. Concurrently the peak to peak deflection must be set to saturate to a constant frequency and yet not buckle or break the sample.

Considering the foregoing factors and noting that J, K_p and D are quite similar from one instrument to another, a critical experiment would be to calibrate the coupled harmonic oscillators with samples of known moduli. By varying I and the slenderness ratio (L/r, where r is the radius of gyration $= \sqrt{I/A}$) *, the reduced plot of the quotient of the actual and the theoretical squares of the frequency vs. EI for several ratios of (L/r) could be generated. In this way the useful working range of these instruments could be mapped out, and a correction factor applied whenever a preferred geometry was not feasible but a quantitative result was desired.

SUMMARY

Occasionally relaxation properties are desired from materials that are neither fluid enough to take advantage of surface tension test methods nor rigid enough to be self-supporting members. For these cases one approach is to test the sample via a superstructure fabricated from a resilient, non-reactive material that responds predictably under test conditions. Consequently, the general relation is derived for the frequency response of two coupled harmonic oscillators. Thereafter the solution for homogeneous beams is considered followed by the non-homogeneous case. Using the transformation technique described, the composite beam is reduced to one material and a new expression derived which describes the sample modulus (E_s) in terms of the difference of the squares of the composite beam (f_c) and the holder frequency (f_h)

$$E_s = \frac{2\pi^2 J(f_c^2 - f_h^2)}{w(D + \frac{1}{2}L)^2}\left(\frac{L}{t}\right)^3$$

* While L/T is adequate for comparing beams of a fixed cross-sectional shape, L/r must be used to yield a general relationship for columns of any configuration. For example, for rectangular prisms rotated about $y = T/2$, $L/r = \sqrt{12}\ L/T$, whereas for cylinders of diameter T rotated about $y = T/2$, $L/r = 4\ L/T$.

To demonstrate this technique the early setting characteristics of a semi-rigid material, dental amalgam, were observed via the utilization of a U-shaped acrylic channel. These moduli results compared favorably with previous literature and with recent compressive test data obtained on these same sections. Here special attention was also given to the error introduced from designing an asymmetrical holder as well as from neglecting the composite beam's moment of inertia.

The discussion concludes with an appraisal of the technique, the factors that must be considered for quantitative analysis, and a suggestion for better defining the instrument's capabilities.

ACKNOWLEDGEMENTS

We wish to thank Dr. D.F. Taylor for his assistance with the preparation of the alloys. This investigation was supported by NIH research grant No. DE02668. RCDA No. DE00052 (R.P.K.) and RFA No. DE05132 (A.R.G.).

REFERENCES

1 L.E. Nielsen, Mechanical Properties of Polymers, Reinhold, New York, 1962, Chap. 7.
2 Thermal Analysis Review: Dynamic Mechanical Analysis, promotional material of the DuPont Instruments Co., Inc.
3 R.L. Hassel and P.S. Gill, Shear Measurements with the Dynamic Mechanical Analyzer, paper presented at the 8th North Am. Therm. Anal. Soc. Conf., Atlanta, 1978.
4 F.W. Sears and M.W. Zemansky, University Physics, Addison-Wesley, Reading, 3rd edn., 1963, Chap. 11.
5 O.W. Eshbach and M Sounders, Handbook of Engineering Fundamentals, Wiley, New York, 3rd edn., 1975, p. 514
6 J.N. Cernica, Strength of Materials, Holt, Rinehart, and Winston, New York, 1966, Chap. 3
7 W.B. Eames and J.F. MacNamara, Oper. Dent., 1 (1976) 98.
8 M.L. Malhotra and K. Asgar, J. Am. Dent. Assoc., 96 (1978) 444.
9 J.W. Osborne, E N. Gale, C.L Chew, B F. Rhodes and R.W. Phillips, J. Dent. Res., 57 (1978) 983.
10 Guide to Dental Material and Devices, American Dental Association, Council on Dental Materials and Devices, Chicago, 7th edn., 1974—1975, p. 170.
11 S. Espevik, Acta Odontol. Scand., 33 (1975) 239.
12 A.J. Spanauf, A.G. Vermeersch and M.M.A. Vrijhoef, Rev. Belge Med. Dent., 31 (1976) 225; 31 (1976) 341.
13 N.O. Taylor, W.T. Sweeney, D.B. Mahler and E.J. Dinger, J. Dent. Res., 28 (1949) 228.
14 D.L. Smith, H J. Caul and W.T Sweeney, J. Am Dent. Assoc., 53 (1956) 677.
15 J.W. Stanford, K.V. Weigel, G.C. Paffenbarger and W.T. Sweeney, J Am. Dent. Assoc., 60 (1960) 746.
16 M.S. Rodriguez and G. Dickson, J. Dent. Res., 41 (1962) 840.
17 G. Dickson and P.L. Oglesby, J. Dent. Res., 46 (1967) 1475.
18 D.E. Grenoble and J.L. Katz, J. Biomed. Mater. Res., 5 (1971) 489.
19 D.E Grenoble and J.L. Katz, J. Biomed. Mater. Res., 5 (1971) 503.
20 J.M. Powers and J.W. Farah, J. Dent. Res., 54 (1975) 902.
21 S. Espevik, Acta Odontol. Scand., 36 (1978) 103.
22 R.P. Kusy, A.R. Greenberg and D.F. Taylor, Dynamic Mechanical Analysis of Amalgam Setting Rates, paper presented at the Int. Assoc. Dent. Res. Meet., New Orleans, 1979.